European Radiology (2021) 31:9198–9210
https://doi.org/10.1007/s00330-021-07909-7

COMPUTED TOMOGRAPHY

Characteristic findings of microvascular dysfunction on coronary computed tomography angiography in patients with intermediate coronary stenosis

Masahiro Hoshino[1] · Seokhun Yang[2] · Tomoyo Sugiyama[1] · Jinlong Zhang[2] · Yoshihisa Kanaji[1] · Rikuta Hamaya[1,3] · Masao Yamaguchi[1] · Masahiro Hada[1] · Tomoki Horie[1] · Kai Nogami[1] · Hiroki Ueno[1] · Toru Misawa[1] · Taishi Yonetsu[4] · Doyeon Hwang[2] · Joo Myung Lee[2] · Eun-Seok Shin[5] · Joon-Hyung Doh[6] · Chang-Wook Nam[7] · Bon-Kwon Koo[2] · Tetsuo Sasano[4] · Tsunekazu Kakuta[1]

Received: 27 August 2020 / Revised: 19 February 2021 / Accepted: 18 March 2021 / Published online: 19 May 2021
© European Society of Radiology 2021

Abstract

Objectives We aimed to assess the prevalence of coexistence of coronary microvascular dysfunction (CMD) in patients with intermediate epicardial stenosis and to explore coronary computed tomography angiography (CCTA)–derived lesion-, vessel-, and cardiac fat–related characteristic findings associated with CMD.

Methods A retrospective cross-sectional single-center study included a total of 177 patients with intermediate stenosis in the left anterior descending artery (LAD) who underwent CCTA and invasive physiological measurements. The 320-slice CCTA analysis included qualitative and quantitative assessments of plaque, vessel, epicardial fat volume (ECFV) and epicardial fat attenuation (ECFA), and pericoronary fat attenuation (FAI). CMD was defined by the index of microcirculatory resistance (IMR) ≥ 25.

Results In the entire cohort, median fractional flow reserve (FFR) and median IMR values were 0.77 (0.69–0.84) and 19.0 (13.7–27.7), respectively. The prevalence of CMD was 32.8 % (58/177) in the total cohort. The coexistence of CMD and functionally significant stenosis was 34.3 % (37/108), whereas CMD in nonsignificant intermediate stenosis was 30.4 % (21/69). CMD was significantly associated with greater lumen volume ($p = 0.031$), greater fibrofatty and necrotic component (FFNC) volume ($p = 0.030$), and greater ECFV ($p = 0.030$), but not with FAI ($p = 0.832$) and ECFA ($p = 0.445$). On multivariable logistic regression analysis, vessel volume, vessel lumen volume, lesion remodeling index, ECFV, and lesion FFNC volume were independent predictors of CMD.

Conclusions The prevalence of CMD was about one-third in patients with intermediate stenosis in LAD regardless of the presence or absence of functional stenosis significance. The integrated CCTA assessment may help in the identification of CMD.

Key Points

- *The coexistence of coronary microvascular dysfunction (CMD) and functionally significant stenosis was 34.3 %, whereas CMD in nonsignificant intermediate stenosis was 30.4 %.*
- *Coronary computed tomography angiography (CCTA)-derived CMD characteristics were vessel volume, vessel lumen volume, remodeling index, epicardial fat volume, and fibrofatty necrotic core volume.*
- *Integrated CCTA assessment may help identify the coexistence of CMD and epicardial stenosis.*

✉ Tsunekazu Kakuta
kaz@joy.email.ne.jp

[1] Division of Cardiovascular Medicine, Tsuchiura Kyodo General Hospital, 4-1-1 Otsuno, Tsuchiura City, Ibaraki 300-0028, Japan

[2] Department of Internal Medicine and Cardiovascular Center, Seoul National University Hospital, Seoul, South Korea

[3] Harvard T.H. Chan School of Public Health, Boston, MA, USA

[4] Department of Cardiovascular Medicine, Tokyo Medical and Dental University, Tokyo, Japan

[5] Department of Cardiology, Ulsan Medical Center, Ulsan Hospital, Ulsan, South Korea

[6] Department of Medicine, Inje University Ilsan Paik Hospital, Goyang, South Korea

[7] Department of Medicine, Keimyung University Dongsan Medical Center, Daegu, South Korea

Keywords Coronary artery disease · Computed tomography angiography · Microcirculation · Myocardial fractional flow reserve · Adipose tissue

Abbreviations

CABG	Coronary artery bypass graft surgery
CAD	Coronary artery disease
CCTA	Coronary computed tomography angiography
CFR	Coronary flow reserve
CMD	Coronary microvascular dysfunction
ECFA	Epicardial fat attenuation
ECFV	Epicardial fat volume
ESS	Endothelial shear stress
FFNC	Fibrofatty and necrotic component
FFR	Fractional flow reserve
IMR	Index of microcirculatory resistance
LAD	Left anterior descending artery
MVD	Microvascular dysfunction
PCI	Percutaneous coronary intervention

Introduction

Ischemia caused by coronary microvascular dysfunction (CMD) exhibits a worse prognosis independent of epicardial stenosis severity [1–3]. There is an emerging recognition that microvascular function plays an important role in patient symptoms and prognosis [4, 5]. For epicardial disease, fractional flow reserve (FFR) is the current standard for the invasive evaluation of coronary flow limitation, but FFR is not capable of assessing the microvascular function. CMD remains a diagnostic challenge for non-invasive imaging [6]. Prior studies reported the coexistence of CMD with atherosclerotic plaques in most patients with coronary artery disease (CAD), resulting in the further difficulty in discriminating the cause of ischemia by non-invasive imaging modalities [2]. Following recent trials, coronary computed tomography angiography (CCTA) has been recommended as a gatekeeper for the assessment of stable chest pain in patients with low to intermediate risk of CAD [7, 8]. The atherosclerotic burden or disease extent in entire epicardial coronary arteries obtained by CCTA provides prognostic information in patients with CAD [9, 10]. CCTA also provides the qualitative and quantitative assessment of the individual component of atherosclerotic plaque and the entire vessel, as well as cardiac mass and epicardial and pericoronary fat assessments [10–13]. However, there has been limited data regarding the prevalence of CMD in patients who underwent the first-line CTCA examination for chest pain and subsequently underwent invasive coronary physiological measurements for intermediate lesions [14]. Although this patient population is one of the typical contemporary clinical scenarios, it is unknown if CCTA provides characteristic findings or diagnostic information regarding CMD.

Therefore, the present study sought to (1) assess the prevalence of CMD in patients with intermediate coronary risk and a single de novo intermediate stenosis in the left anterior descending artery (LAD) on CCTA by stratifying using FFR and the index of microcirculatory resistance (IMR), and (2) explore the CCTA-derived lesion-, vessel-specific, and cardiac fat–related findings associated with CMD.

Materials and methods

Study design and patient population

The present study is the substudy of the multicenter study CCTA-FFR Registry for Risk Prediction, Clinical Trial Registration Information: NCT04037163, and the study population was derived from the institutional CCTA registry of Tsuchiura Kyodo General Hospital, one of the cardiac centers that participated in the aforementioned international multicenter registry. For this study, we retrospectively investigated lesions with angiographically intermediate stenosis (30–80 % diameter stenosis in LAD by visual estimation on CCTA). Cases with a single de novo proximal lesion on CCTA were included and assessed in the present study. All data except for the epicardial and pericoronary fat analysis were collected at the core laboratories, and independent screening and analyses were performed for angiographic and CCTA data. The patients with depressed left ventricular systolic function (ejection fraction < 35 %), previous coronary artery bypass graft surgery (CABG), chronic renal disease, chronic total occlusion lesions, left main disease, abnormal epicardial coronary flow (TIMI flow < 3), or planned CABG after diagnostic angiography were excluded. The indication of CCTA was in accordance with the Appropriate Use Criteria for Cardiac Computed Tomography [15]. Thus, a total of 177 LAD in 177 patients were retrospectively studied in the present study (Fig. 1). All these patients underwent invasive coronary physiological assessment within 90 days after CCTA. This study was conducted in compliance with the institutional ethics committee guidelines and received its approval. The present study also complied with the Declaration of Helsinki for investigation in human beings, and all patients provided written informed consent for future data utilization before enrollment.

CCTA and analysis of plaque characteristics

All CCTAs were performed according to the Society of Cardiovascular Computed Tomography guidelines [16]. The

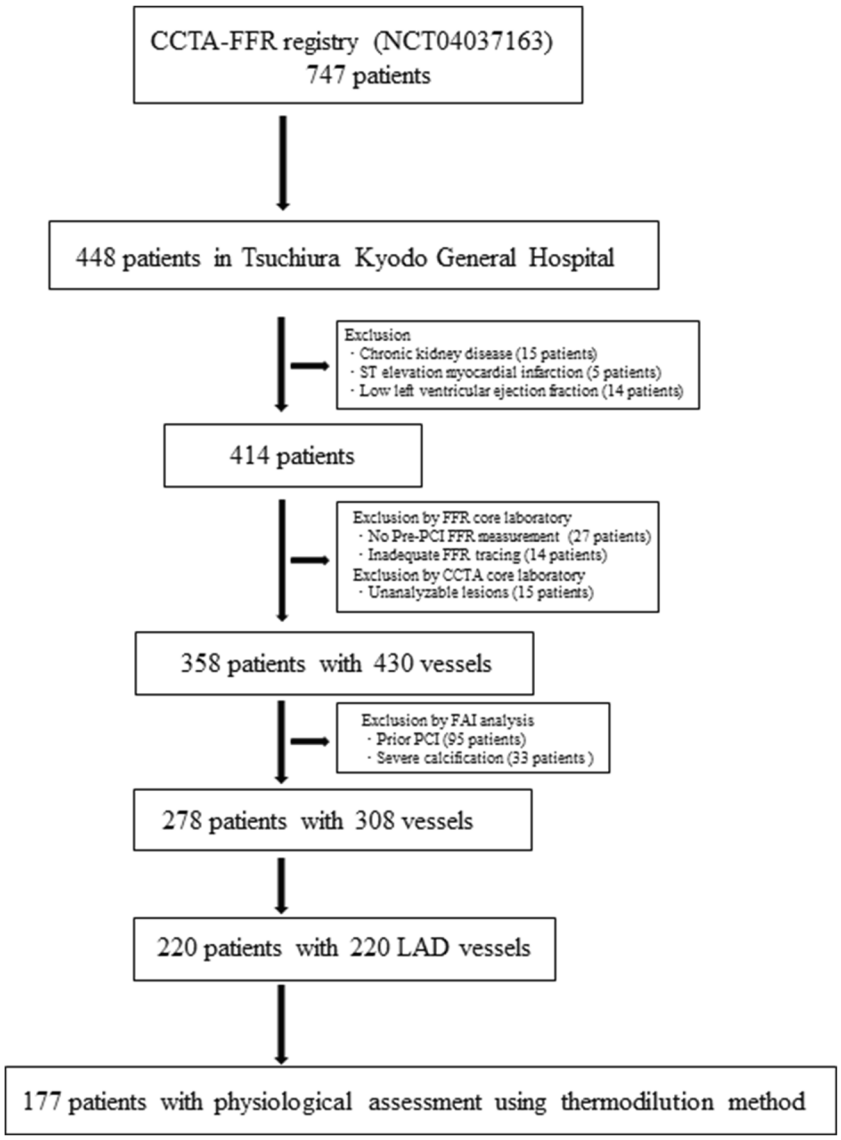

Fig. 1 Study flow diagram. CCTA, coronary computed tomography angiography; CAG, coronary angiography; PCI, percutaneous coronary intervention; FFR, fractional flow reserve; FAI, pericoronary fat attenuation; LAD, left anterior descending artery

CCTA images were analyzed at a core laboratory in a blinded manner (Severance Cardiovascular Hospital) to obtain qualitative and quantitative stenosis and plaque features by expert CCTA readers. CCTA analysis was performed in 3 steps. First, qualitative plaque characteristics were analyzed according to the definitions from previous studies [17–19]. Second, cross-sectional quantitative analysis of target stenosis, including minimum lumen area (MLA), plaque burden, and area stenosis, was performed as previously described [19]. Third, the 3-dimensional (3-D) plaque quantification was performed for target stenosis and target vessels [20, 21], using semiautomated plaque analysis software (QAngioCT Research Edition version 2.1.9.1, Medis Medical Imaging Systems) with appropriate manual correction [22]. For plaque quantification in the whole vessel, total plaque volume and fibrofatty and necrotic component (FFNC) volume were selected as clinically relevant parameters from previous studies [20, 23, 24].

Epicardial fat, pericoronary fat, and pericoronary fat attenuation (FAI)

ECFV and ECFA were measured offline from CCTA images using cardiac risk analysis software (VirtualPlace, AZE Inc.) as previously described [25]. In brief, ECFV was assessed by manual tracing of the pericardial sac as an outer border in axial planes from the right pulmonary artery to the apex of the heart for quantification. CT attenuation range of epicardial fat was set between −190 and −30 Hounsfield Unit (HU). After the 3-D reconstruction, ECFV was automatically calculated by the software program. ECFA was automatically calculated by the software (VirtualPlace, AZE Inc.) as mean Hounsfield Units of all

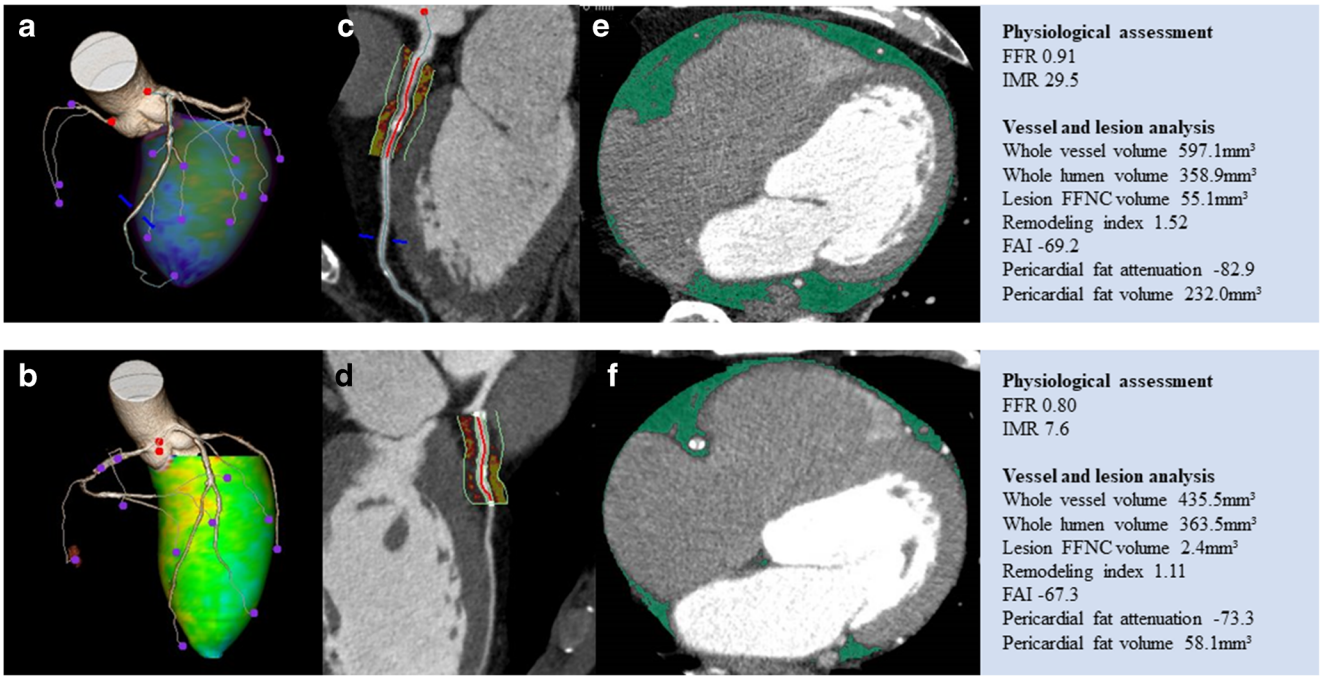

Fig. 2 A representative case of CCTA assessment. Lesions were classified according to IMR values. **a** CMD: Lesion with IMR ≥ 25. **b** Non-CMD: Lesion with IMR < 25. **c** FAI in lesion with CMD. **d** FAI in lesion with non-CMD. **e** ECFV and ECFA in lesion with CMD. **f** ECFV and ECFA in lesion with non-CMD. IMR, index of microcirculatory resistance; CMD, coronary microvascular dysfunction; ECFV, epicardial fat volume; ECFA, epicardial fat attenuation; FFNC, fibrofatty and necrotic component. Other abbreviations as in Fig. 1

pixels defined as ECFV. Representative images are shown in Fig. 2. Pericoronary fat attenuation (FAI) analysis was performed using a dedicated workstation (Aquarius iNtuition Edition version 4.4.13.P3; TeraRecon Inc.). A detailed description of the CCTA acquisition and the CCTA analysis is presented in the Supplemental Materials.

Invasive coronary angiography and physiological assessments

Physiological parameters including FFR, IMR, and coronary flow reserve (CFR) were obtained using a single 0.014-inch PressureWire™ (Abbott Vascular). (The details are shown in Supplemental Table.) After wire calibration, the intracoronary pressure distal to the coronary stenosis was measured. Subsequently, 3 mL room-temperature saline was administered three times, and the resting mean transit time (Tmn) was determined. For both measurements, maximal hyperemia was induced by intravenous infusion of adenosine 5′-triphosphate (160 $\mu g \cdot kg^{-1} \cdot min^{-1}$). FFR was calculated as the ratio of mean distal coronary to aortic pressure (Pd/Pa) during maximum hyperemia. CFR was defined as resting Tmn divided by hyperemic Tmn. IMR was defined as hyperemic (Pa × Tmn × ([1.35 × Pd / Pa] − 0.32) [26]. Physiological assessments were performed by five board-qualified cardiologists who had at least 300 cases of FFR/IMR measurements and analyzed by two independent doctors in Tsuchiura Kyodo General Hospital (M.H. and T.S.) who were blinded to the patients' data including baseline characteristics, angiographic, and CCTA findings.

Statistical analysis

The statistical analysis was performed using SPSS version 25.0 (SPSS, Inc.) and R version 3.5.3. Categorical data were expressed as numbers and percentages and compared by chi-square or Fisher's exact tests, as appropriate. The normality of the distribution of the values was assessed by Shapiro-Wilk statistics. Continuous data were expressed as mean ± standard deviation (SD) or median (interquartile range [IQR]) and analyzed using the Mann–Whitney test and the variance for variables with non-normal distribution and normal distribution, respectively. Clinical characteristics, CCTA-derived qualitative and quantitative data, and physiological indices were compared between 4 groups classified by FFR and IMR cutoffs (FFR = 0.80, IMR = 25, respectively) using the Kruskal-Wallis test. Receiver operating characteristics (ROC) curve analysis was performed to assess the best cutoff values for predicting FFR ≤ 0.80 and IMR ≥ 25. The optimal cutoff value was calculated using the Youden index. Univariable and multivariable linear regression analyses were performed to determine predictive factors

of IMR values. Univariable and multivariable logistic regression analysis was performed to identify the predictive factors of IMR ≥ 25 [27]. A collinearity index was used to evaluate the linear collinearity between covariates with the Akaike information criterion to avoid overfitting. The associated variables in univariable analyses (p < 0.10) were entered into the multivariable model. The Hosmer-Lemeshow statistic was applied to assess model calibration. The prediction models for IMR ≥ 25 were constructed to determine the incremental discriminatory and reclassification performance of clinical risk factors and CT variables using relative integrated discrimination improvement (IDI) and category-free net reclassification index (NRI). As a baseline reference, clinical model 1 included clinical characteristics such as age, sex, hypertension, diabetes mellitus, and hyperlipidemia; then, we tested CCTA variables added to the clinical model. A 2-tailed value of p < 0.05 was considered statistically significant.

Results

Baseline patient characteristics, angiographic, physiological, and CCTA findings

Baseline clinical, angiographic, physiological, and CCTA findings in 4 groups stratified by the cutoff values of FFR = 0.80 and IMR = 25 are summarized in Tables 1 and 2. In a total cohort, the median age was 68 (62–74) years, and 132/177 (74.6 %) were male. The median % diameter stenosis, FFR, CFR, and IMR were 51.4 (37.7–61.0) %, 0.77 (0.69–0.84), 2.25 (1.51–3.51), and 19.0 (13.7–27.7), respectively. The prevalence of CMD was 32.8 % (58/177). The coexistence of CMD and functionally significant stenosis was 34.3 % (37/108). In contrast, CMD in nonsignificant intermediate stenosis was 30.4 % (21/69), indicating no significant difference in the prevalence of CMD regardless of the presence or absence of functionally significant stenosis (p = 0.716). No significant relationship was detected between FFR and IMR (p = 0.882). Of note, ECFV and FAI showed an inverse relationship (Fig. 3a). ECFV and ECFA similarly showed the inverse relationship (Fig. 3b). There was a significant linear relationship between FAI and ECFA (Fig. 3c).

CCTA findings and the presence of CMD

The results of univariable and multivariable linear regression analyses to predict IMR values are shown in Table 3. On multivariable analysis, whole vessel lumen volume, remodeling index, and ECFV remained significant. A significant albeit weak relationship was observed between IMR and ECFV (R = 0.181, p = 0.017). The calcium score of LAD showed no significant relationship with IMR.

CMD was significantly associated with smaller whole vessel volume, greater whole vessel lumen volume, greater lesion remodeling index, lesion FFNC volume, and greater ECFV, but not with FAI. On multivariable regression analysis, whole vessel volume (odds ratio [OR] 0.996, p = 0.017), whole vessel lumen volume (OR 1.01, p = 0.003), remodeling index (OR 2.89, p = 0.029), ECFV (OR 1.01, p = 0.020), and lesion FFNC volume (OR 1.01, p = 0.007) were independent predictors of CMD (Table 4). Hosmer-Lemeshow statistic indicated a significant fitness of this model (p = 0.834).

Discrimination capability of CCTA findings for CMD

The addition of CCTA-derived factors to the risk model based on clinical characteristics significantly improved the predictive ability of the presence of CMD (Table 5). Further consideration of ECFV provided the significant incremental predictive capability for the presence of CMD (Table 5).

ROC analysis revealed the best cutoff values for predicting CMD as follows: remodeling index ≥ 1.36 (area under the curve [AUC] 0.588, 95 % confidence interval [CI] 0.496–0.679, p = 0.056), lesion FFNC volume ≥ 107.8 mm^3 (AUC 0.601, 95 % CI 0.512–0.689, p = 0.030), and ECFV ≥ 129.6 mm^3 (AUC 0.601, 95 % CI 0.511–0.690, p = 0.030). When the total cohort was divided into four groups according to the numbers of the aforementioned CCTA-derived risk factors of CMD, considering the numbers of risks assessed by each best cutoff values of remodeling index, lesion FFNC volume, and ECFV, the territories with all of these CMD risk factors showed 100 % prevalence of CMD. In contrast, the territories without these factors presented a significantly reduced prevalence of CMD (p < 0.001; Fig. 4).

Discussion

The current study investigated the prevalence of CMD in the patients with a single de novo intermediate lesion (30–80 % by CCTA visual estimation) in LAD. The first-line non-invasive imaging test was CCTA as the guideline-recommended contemporary routine practice, indicating the typical cohort who subsequently underwent invasive or non-invasive functional testing. The main findings were as follows: (1) the prevalence of CMD in the total cohort was 32.8 %; (2) the coexistence of CMD and functionally significant stenosis was 34.3 %, whereas the prevalence of CMD in patients with nonsignificant LAD stenosis was 30.4 % (p = 0.716, vs. CMD with significant stenosis); (3) CCTA-derived characteristic features including vessel volume, lumen volume, remodeling index, ECFV, and FFNC volume were identified to be independently associated with the presence of CMD; (4) the integrated

Table 1 Patient characteristics

	Overall (N = 177)	FFR ≤ 0.80 and IMR ≥ 25 (N = 37)	FFR ≤ 0.80 and IMR < 25 (N = 71)	FFR > 0.80 and IMR ≥ 25 (N = 21)	FFR > 0.80 and IMR < 25 (N = 48)	p value
Age, y	68.0 (62.0–74.0)	63.0 (57.0–73.0)	68.0 (63.0–73.5)	71.0 (64.0–73.0)	68.0 (64.0–74.0)	0.194
Male	132 (74.6)	32 (86.5)	57 (80.3)	15 (71.4)	28 (58.3)	**0.015**
BMI, $kg{\cdot}m^{-2}$	24.6 ± 3.3	25.3 ± 3.8	24.3 ± 3.3	24.5 ± 3.2	24.4 ± 3.0	0.532
Hypertension	132 (74.6)	30 (81.1)	49 (69.0)	18 (85.7)	35 (72.9)	0.356
Diabetes mellitus	55 (31.1)	14 (37.8)	22 (31.0)	6 (28.6)	13 (27.1)	0.751
Hyperlipidemia	105 (59.3)	24 (64.9)	40 (56.3)	12 (57.1)	29 (60.4)	0.850
eGFR, $mL{\cdot}min^{-1}{\cdot}1.73\ m^{-2}$	70.3 (62.5–79.9)	70.9 (63.6–82.5)	69.1 (61.1–78.2)	69.0 (60.8–73.1)	73.4 (65.1–80.9)	0.569
NT-proBNP, $pg{\cdot}mL^{-1}$	116.0 (55.0–284.8)	109.0 (40.0–310.0)	112.0 (55.0–284.8)	177.0 (113.0–284.8)	110.0 (54.8–252.7)	0.685
Ejection fraction, %	66.0 (60.8–71.0)	67.0 (62.5–71.5)	66.0 (59.3–71.0)	66.0 (56.0–69.0)	66.0 (62.8–71.0)	0.601
Physiological indices						
FFR	0.77 (0.69–0.84)	0.70 (0.60–0.74)	0.72 (0.64–0.76)	0.86 (0.83–0.88)	0.86 (0.83–0.88)	**< 0.001**
CFR	2.25 (1.51–3.51)	1.43 (1.10–1.97)	2.61 (2.02–3.42)	1.98 (1.55–3.13)	3.70 (2.25–5.34)	**< 0.001**
IMR	19.0 (13.7–27.7)	33.2 (27.2–38.9)	15.7 (11.9–19.1)	35.0 (29.7–40.7)	14.1 (11.2–19.0)	**< 0.001**
Tmn at rest	0.87 (0.61–1.21)	1.10 (0.85–1.50)	0.80 (0.53–1.04)	1.01 (0.89–1.55)	0.77 (0.48–1.03)	**< 0.001**
Tmn at hyperemia	0.33 (0.23–0.55)	0.65 (0.56–0.99)	0.31 (0.23–0.40)	0.49 (0.38–0.59)	0.22 (0.16–0.27)	**< 0.001**
Angiographic characteristics						
Reference diameter, mm	2.7 (2.3–3.0)	2.6 (2.3–3.0)	2.6 (2.2–3.0)	2.7 (2.3–3.1)	2.7 (2.4–3.1)	0.856
Minimum lumen diameter, mm	1.3 (1.0–1.7)	1.2 (1.0–1.4)	1.1 (0.9–1.4)	1.7 (1.1–2.0)	1.6 (1.4–1.9)	**< 0.001**
Diameter stenosis, %	51.4 (37.7–61.0)	54.9 (49.9–61.3)	56.7 (46.1–66.3)	44.5 (27.3–54.5)	39.4 (29.3–50.4)	**< 0.001**
Lesion length, mm	11.2 (8.5–16.2)	12.3 (8.7–22.5)	12.8 (9.2–19.4)	10.7 (6.2–13.9)	9.1 (6.3–13.4)	**0.003**

Data are presented as n (%), mean ± SD or median (interquartile range). Bolded p values indicate statistical significance ($p < 0.05$)

BMI body mass index, *eGFR* estimated glomerular filtration rate, *NT-proBNP* N-terminal pro-B-type natriuretic peptide, *FFR* fractional flow reserve, *CFR* coronary flow reserve, *IMR* index of microcirculatory resistance, *Tmn* mean transit time

Table 2 Whole vessel quantification, lesion characteristics, and cardiac mass by CCTA

	Overall ($N = 177$)	FFR ≤ 0.80 and IMR ≥ 25 ($N = 37$)	FFR ≤ 0.80 and IMR < 25 ($N = 71$)	FFR > 0.80 and IMR ≥ 25 ($N = 21$)	FFR > 0.80 and IMR < 25 ($N = 48$)	*p* value
Per-vessel analysis						
Vessel volume, mm^3	745.4 (578.4–974.9)	814.7 (610.9–999.9)	711.4 (566.9–892.5)	803.3 (636.9–1134.7)	750.2 (561.0–960.5)	0.211
Lumen volume, mm^3	551.9 (424.1–702.1)	605.5 (392.8–785.4)	511.1 (379.6–614.1)	657.6 (471.8–848.0)	555.4 (438.5–700.9)	**0.026**
Whole vessel mass volume, mm^3	53.7 (44.9–66.2)	55.9 (48.8–73.0)	56.0 (45.4–70.7)	50.3 (45.6–56.9)	49.9 (41.1–61.0)	**< 0.001**
Plaque volume, mm^3	189.6 (99.3–278.2)	202.8 (129.5–304.7)	203.2 (125.8–283.8)	162.1 (55.2–233.9)	137.9 (92.1–244.8)	0.096
Fibrous volume, mm^3	77.4 (43.7–123.7)	88.0 (54.9–130.6)	94.7 (49.4–125.7)	72.8 (32.8–112.9)	57.8 (37.4–114.1)	0.242
FFNC volume, mm^3	33.4 (11.2–72.9)	55.6 (21.4–114.8)	42.1 (15.7–72.5)	27.4 (14.9–55.1)	17.1 (5.9–47.6)	**0.003**
Dense calcium volume, mm^3	43.1 (9.8–90.9)	36.0 (6.3–71.8)	42.6 (12.2–95.5)	18.8 (4.6–84.4)	53.4 (16.6–97.0)	**< 0.001**
Plaque burden mean, %	35.6 (27.5–44.7)	37.1 (30.9–44.7)	40.1 (30.7–48.7)	27.1 (22.4–35.6)	31.0 (24.3–38.1)	**< 0.001**
Agatston score	149.2 (36.4–307.8)	101.6 (25.1–268.8)	189.8 (62.3–394.0)	119.0 (14.2–210.5)	163.1 (41.8–293.8)	0.202
Plaque analysis						
Vessel volume, mm^3	419.3 (258.9–566.6)	453.4 (278.7–691.1)	438.5 (285.5–548.0)	361.3 (174.8–634.1)	379.8 (253.5–498.0)	0.629
Lumen volume, mm^3	229.1 (148.8–322.4)	237.2 (142.2–356.3)	215.8 (154.6–303.0)	229.1 (130.7–400.3)	237.8 (172.8–306.2)	0.688
Plaque volume, mm^3	160.0 (81.4–262.5)	202.8 (124.3–305.6)	194.4 (97.3–277.5)	102.6 (38.7–233.8)	102.8 (69.2–217.0)	**0.043**
Lesion maximal plaque thickness	2.01 (1.66–2.63)	2.40 (1.80–2.99)	2.09 (1.74–2.63)	1.81 (1.47–2.547)	1.83 (1.62–2.24)	**0.025**
MLA, mm^2	2.0 (1.5–3.0)	1.9 (1.6–2.5)	1.7 (1.2–2.4)	3.2 (1.8–4.5)	2.7 (2.0–3.9)	**< 0.001**
Plaque eccentricity	1.00 (0.77–1.00)	1.00 (0.80–1.00)	1.00 (0.64–1.00)	1.00 (0.72–1.00)	1.00 (0.99–1.00)	0.086
Remodeling index	1.09 (0.88–1.33)	1.14 (0.92–1.58)	1.09 (0.88–1.28)	1.07 (0.97–1.45)	1.07 (0.84–1.27)	0.273
Low attenuation plaque	47 (26.6)	13 (35.1)	26 (36.6)	4 (19.0)	4 (8.3)	**0.003**
Spotty calcification	19 (10.7)	6 (16.2)	9 (12.7)	1 (4.8)	3 (6.2)	0.404
Fibrous plaque volume, mm^3	65.8 (28.8–113.7)	88.0 (50.8–131.2)	82.3 (41.0–121.5)	55.9 (20.4–112.8)	46.6 (25.5–95.5)	0.100
FFNC volume, mm^3	27.0 (7.8–69.9)	55.6 (17.4–114.8)	34.6 (10.2–71.7)	22.6 (14.9–47.9)	16.0 (2.4–37.7)	**< 0.001**
Plaque burden, %	75.6 (60.3–84.8)	83.4 (61.0–87.3)	78.5 (66.3–88.0)	71.0 (60.3–78.7)	61.2 (50.3–75.7)	**< 0.001**
Fat analysis						
FAI	− 71.8 (− 78.0 to -67.9)	− 72.7 (− 77.2 to -67.1)	− 70.4 (− 76.5 to -66.8)	− 71.4 (− 79.6 to -69.4)	− 74.4 (− 79.3 to − 68.9)	0.395
ECFA	− 76.0 (− 79.2 to − 72.6)	− 76.1 (− 79.2 to − 72.7)	− 76.0 (− 78.6 to − 71.7)	− 76.0 (− 80.7 to − 74.4)	− 75.8 (− 79.4 to − 72.8)	0.786
ECFV, mm^3	98.7 (74.7–133.0)	107.0 (88.2–139.4)	95.4 (69.2–125.1)	106.3 (88.1–145.8)	93.8 (74.4–121.6)	0.191

Data are presented as *n* (%) or median (interquartile range). Bolded *p* values indicate statistical significance ($p < 0.05$)

CCTA coronary computed tomography angiography, *FFNC* fibrofatty and necrotic core component, *MLA* minimum lumen area, *FAI* pericoronary fat attenuation, *ECFA* epicardial fat attenuation, *ECFV* epicardial fat volume. Other abbreviations as in Table 1

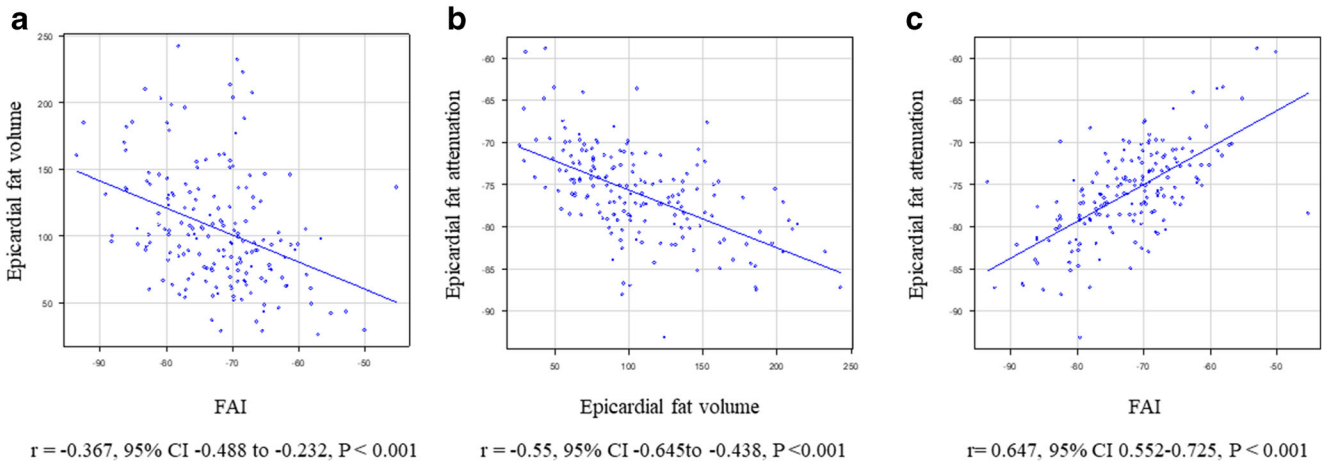

Fig. 3 Correlation analysis between epicardial fat and FAI. Correlation analyses between ECFV and FAI (**a**), ECFV and ECFA (**b**), and ECFA and FAI (**c**). Abbreviations as in Figs. 1 and 2

assessment of CCTA may help identify or discriminate the presence of CMD in the present study population.

To our knowledge, this is the first study to explore the characteristic CCTA findings to be associated with the presence of CMD. The present study also assessed the prevalence of CMD in relation to the presence or absence of functionally significant epicardial stenosis evaluated by FFR in patients with stable CAD with intermediate stenosis in LAD.

Our results indicated that about one-third of the patients with functionally significant stenosis in LAD treated with subsequent percutaneous coronary intervention (PCI) according to the current guidelines showed the coexistence of CMD. Recent evidence strongly suggests the coexistence of CMD and atherosclerosis in patients with CAD [2]. However, no specific therapeutic strategy for CAD patients has been proposed according to the presence or absence of the coexisting CMD. After successful PCI, anginal symptoms may still sustain in patients by the remaining CMD. It has been reported that, even in the presence of functionally significant epicardial stenosis, CMD holds prognostic information [3]. A recent study has reported that CMD is relatively rare in the absence of obstructive disease in the symptomatic population with suspicion of stable CAD [28]. The authors concluded that CMD was closely associated with the presence of epicardial coronary atherosclerosis in patients with suspected CAD, demonstrating that 88 % of the patients with CMD had evidence of atherosclerosis, and 59 % showed evidence of the coexistence of obstructive CAD. However, FFR measurement was performed only in selected cases. A recent study using an intracoronary pressure wire has also reported that nonobstructive CAD was not uncommon (39 %) in symptomatic patients with suspicion or known CAD [29]. Our results are in line with these results. Given the reported

Table 3 Univariable and multivariable linear regression analysis for IMR

	Univariable analysis			Multivariable analysis		
	β	95% CI	*p* value	*β*	95% CI	*p* value
Age	− 0.10	− 0.28 to 0.09	0.298			
Male	0.95	− 2.97 to 4.78	0.634			
BMI	0.35	− 0.16 to 0.86	0.180			
Whole vessel volume	0.01	− 0.000 to 0.011	0.051	− 0.01	− 0.02 to 0.002	0.092
Whole lumen volume	0.01	0.002–0.017	**0.009**	0.02	0.004–0.032	**0.010**
Remodeling index	6.42	2.35–10.50	**0.002**	7.40	3.36–11.44	**< 0.001**
ECFV	0.05	0.01–0.08	**0.017**	0.05	0.012–0.09	**0.010**
Lesion FFNC volume	0.51	0.07–0.95	**0.023**			

CI confidence interval. Other abbreviations as in Tables 1 and 2. Bolded *p* values indicate statistical significance ($p < 0.05$)

Table 4 Univariable and multivariable logistic regression analysis of predicting lesion with IMR ≥ 25

	Univariable analysis			Multivariable analysis		
	OR	95% CI	*p* value	OR	95% CI	*p* value
Age	0.97	0.94–1.01	0.115			
Male	1.71	0.79–3.68	0.171			
BMI	1.06	0.97–1.17	0.217			
Hypertension	2.22	1.06–4.68	**0.036**			
Whole vessel volume	1.00	1.00–1.00	**0.026**	0.996	0.993–0.999	**0.017**
Whole lumen volume	1.00	1.00–1.00	**0.009**	1.01	1.00–1.01	**0.003**
Remodeling index	2.80	1.24–6.31	**0.013**	2.89	1.11–7.52	**0.029**
ECFV	1.01	1.00–1.02	**0.025**	1.01	1.00–1.02	**0.020**
Lesion FFNC volume	1.01	1.00–1.01	**0.011**	1.01	1.00–1.02	**0.007**

OR odds ratio. Other abbreviations as in Tables 1 to 3. Bolded *p* values indicate statistical significance ($p < 0.05$)

significant association of risk factors between CMD and atherosclerosis, it is plausible to consider that the patients with functionally significant stenosis may also have CMD [30, 31].

CMD has been increasingly recognized and showed a broad spectrum as coexistence with coronary atherosclerosis [32]. There is growing evidence that the presence of CMD and its severity may be linked with worse outcomes [32]. Revascularization may not impact on the natural course of CMD. The severity of CMD and epicardial functional severity of CAD evaluated FFR may be distributed in a broad spectrum. The combined effects of epicardial stenosis and CMD and their impact on prognosis may shed light on the management of CAD patients and guidance of the therapeutic benefit of revascularization [32]. The impact of the remaining CMD after revascularization of the significant lesions on symptoms and prognosis should be studied in the large prospective trials. Further studies are needed to facilitate the specific therapeutic strategy in these patients with the coexistence of CMD and coronary artery stenosis.

The association between CCTA characteristics and microvascular dysfunction

The underlying mechanisms leading to atherosclerosis development in patients with CAD are likely to be multifactorial. Both structural and functional abnormalities of the coronary microcirculation may also be involved. A previous study revealed that coronary segments in arteries with abnormal microvascular function exhibited lower endothelial shear stress (ESS) than in arteries with normal microvascular function [33]. Since coronary regions exposed to low ESS are associated with high-risk plaque phenotype [34, 35], lesions with CMD might coexist with vulnerable plaque features such as positive remodeling and FFNC volume identified as CCTA-derived characteristics relevant to CMD in the present study.

Table 5 Prediction model for CMD

Prediction model	*C* statistics	*p* value	IDI	*p* value	NRI	*p* value
Clinical model 1	0.605	-	Reference	-	Reference	-
Clinical model 2	0.717	0.011	0.124	**< 0.001**	0.545	**< 0.001**
Clinical model 3	0.744	0.002	0.162	**< 0.001**	0.601	**< 0.001**
Clinical model 2	0.717	-	Reference	-	Reference	-
Clinical model 3	0.744	0.214	0.038	**< 0.001**	0.519	**< 0.001**

Clinical model 1 (age + male + hypertension + diabetes mellitus + hyperlipidemia)

Clinical model 2 (age + male + hypertension + diabetes mellitus + hyperlipidemia + CCTA vessel and plaque findings)

Clinical model 3 (age + male + hypertension + diabetes mellitus + hyperlipidemia + CCTA vessel and plaque findings + epicardial fat volume)

CMD coronary microvascular dysfunction, *IDI* integrated discrimination improvement, *NRI* net reclassification index, *CCTA* coronary computed tomography angiography

CCTA vessel and plaque findings; whole vessel volume + whole lumen volume + lesion FFNC volume + remodeling index

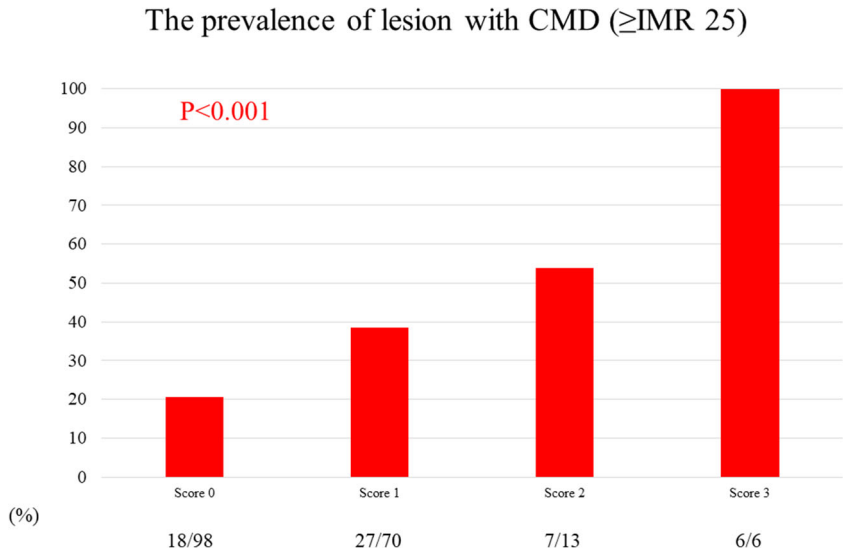

Fig. 4 The prevalence of vessels with CMD according to the CMD risk score. According to the numbers of CCTA-derived risk factors of CMD, using the cutoff values of epicardial fat volume, FFNC volume, and remodeling index, the CMD risk score was calculated (score, 0–3). As the CMD risk score increased, the prevalence of vessels with CMD significantly increased. Abbreviations as in Figs. 1 and 2

Our findings are in accordance with the reports mentioned above and further demonstrated that ECFV and FFNC volume could be associated with the presence of CMD. Several studies have shown the ECFV may be a strong risk factor for CAD [36]. Nappi et al reported, in patients with suspected CAD, ECFV predicts hyperemic myocardial blood flow and reduced myocardial perfusion reserve, confirming that pericardial fat may influence coronary vascular function [37]. Thus, the present study demonstrated that epicardial fat evaluation has a potential role in identifying CMD, although our results are hypothesis-generating. Since this study is cross-sectional, these results may only suggest the inter-relationship of risk factors between CAD and CMD. Further studies are needed to confirm the relationship between epicardial fat and coronary microvascular dysfunction.

The invasive measurement of IMR as a marker of microvascular dysfunction

IMR is an additional invasive metric that has been proposed to examine the presence of microvascular dysfunction (MVD), and it has been defined as distal coronary pressure divided by the inverse of the hyperemic mean transit time (a correlate to absolute flow). Fearon et al reported IMR correlates with a standard experimental method for measuring microcirculatory resistance [38]. Lee et al [27] reported that about a quarter of vessels with FFR ≤ 0.80 have elevated IMR, consistent with MVD diagnosis and in accordance with our results (30.4 % in the present study). Lee also reported that, in patients with nonobstructive LAD, CMD defined as elevated IMR was found to be 20 % [39]. Kobayashi et al reported that clinical factors and epicardial coronary disease severity are not predictors of the extent of CMD in the 3-vessel IMR studies [40]. Our results are in accordance with these results, and extended further that CCTA-derived CMD characteristic features are present and may help identify patients at high risk for CMD-related worse outcomes.

The clinical implication of CCTA in CMD assessment

Following the recent trials [7, 8], CCTA has been recommended as a gatekeeper of the non-invasive testing for the assessment of stable CAD. However, these trials mainly studied epicardial stenosis, and no evaluation of CMD has not been performed. Therefore, the prevalence of CMD in the study population or the prevalence of CMD with or without functionally significant stenosis is unknown. Although significant factors to predict MVD using CCTA were identified in the present study, our results indicated that predicting MVD is still challenging with a *c* statistics of 0.74 by the integrated CCTA assessment. Currently, no diagnostic capability was reported by CCTA combined with clinical baseline characteristics, echocardiography, and electrocardiography for identifying elevated IMR in patients with CAD showing no obstructive epicardial CAD [27]. Our results are first to suggest the capability of CCTA to help determine the presence of MVD independent of functional severity defined by FFR values. The advantage of CCTA is its wide availability and the accurate predictability of FFR. Our results suggest that CCTA may help CMD detection by the currently used routine protocol. Further extensive studies are needed to test our hypothesis-generating results and evaluate the prognostic information of CCTA-derived characteristics of CMD independent of epicardial functional stenosis significance.

Limitations

This study was a retrospective post hoc analysis of existing data, and the influence of potential selection bias could not be

excluded. However, our study's strength is that all data were performed by the same CT modality (320 detector row), and data analysis was managed by the independent core laboratories. Because of the limited number of the entire population of the present study which would preclude extensive subgroup analysis, we tried to exclude reported confounders for IMR- and CT-derived attenuation values. The previous reports demonstrated the difference in microvascular resistance according to the cardiac mass [41]. The difference in IMR according to the lesion location has been also reported [42]. FAI values have been reported to be highest in left circumflex artery [43]. Considering all these reasons, we limited the present assessment in cases with LAD lesions. Therefore, it remains elusive if our findings can be extrapolated to other coronary arteries. A control group of patients without chest pain or evidence of atherosclerosis was not included in the present study. Therefore, the prevalence of CMD in asymptomatic patients without atherosclerosis cannot be compared with the results of the present study population.

Conclusion

The current study investigated the prevalence of CMD in the patients with a single de novo intermediate lesion (30–80 % by visual estimation) detected by CCTA in LAD. About one-third of the present cohort showed the coexistence of CMD and functionally significant stenosis, whereas the prevalence of CMD in patients with nonsignificant stenosis was also not uncommon. CCTA-derived characteristic features associated with CMD may help identify the presence of CMD.

Supplementary Information The online version contains supplementary material available at https://doi.org/10.1007/s00330-021-07909-7.

Funding This study has received funding by an unrestricted research grant from St. Jude Medical (Abbott Vascular) (Santa Clara, CA, USA). The company had no role in study design, conduct, data analysis, or manuscript preparation.

Declarations

Guarantor The scientific guarantor of this publication is Dr. Tsunekazu Kakuta.

Conflict of interest The authors of this manuscript declare relationships with the following companies: Dr. Bon-Kwon Koo received an institutional research grant from St. Jude Medical (Abbott Vascular) and Philips Volcano. Dr. Joo Myung Lee received a research grant from St. Jude Medical (Abbott Vascular) and Philips Volcano. All other authors declare that there is no conflict of interest relevant to the submitted work.

Statistics and biometry One of the authors has significant statistical expertise.

Dr. Rikuta Hamaya kindly provided statistical advice for this manuscript.

Informed consent Written informed consent was obtained from all patients in this study.

Ethical approval Institutional Review Board approval was obtained.

Study subjects or cohorts overlap The present study is the substudy of the multicenter study CCTA-FFR Registry for Risk Prediction, Clinical Trial Registration Information: NCT04037163, and the study population was derived from the institutional CCTA registry of Tsuchiura Kyodo General Hospital, one of the cardiac centers that participated in the aforementioned international multicenter registry. Some study subjects have been previously reported in J Cardiovasc Comput Tomogr. 2020 Feb 6:S1934-5925(19)30733-6.

Methodology
- retrospective
- cross-sectional multicenter study

References

1. Gupta A, Taqueti VR, van de Hoef TP et al (2017) Integrated noninvasive physiological assessment of coronary circulatory function and impact on cardiovascular mortality in patients with stable coronary artery disease. Circulation 136:2325–2336
2. Taqueti VR, Hachamovitch R, Murthy VL et al (2015) Global coronary flow reserve is associated with adverse cardiovascular events independently of luminal angiographic severity and modifies the effect of early revascularization. Circulation 131:19–27
3. Ziadi MC, Dekemp RA, Williams KA et al (2011) Impaired myocardial flow reserve on rubidium-82 positron emission tomography imaging predicts adverse outcomes in patients assessed for myocardial ischemia. J Am Coll Cardiol 58:740–748
4. Jespersen L, Hvelplund A, Abildstrom SZ et al (2012) Stable angina pectoris with no obstructive coronary artery disease is associated with increased risks of major adverse cardiovascular events. Eur Heart J 33:734–744
5. Maddox TM, Stanislawski MA, Grunwald GK et al (2014) Nonobstructive coronary artery disease and risk of myocardial infarction. JAMA 312:1754–1763
6. Mathew RC, Bourque JM, Salerno M, Kramer CM (2020) Cardiovascular imaging techniques to assess microvascular dysfunction. JACC Cardiovasc Imaging 13:1577–1590
7. SCOT-HEART investigators (2015) CT coronary angiography in patients with suspected angina due to coronary heart disease (SCOT-HEART): an open-label, parallel-group, multicentre trial. Lancet 385:2383–2391
8. Douglas PS, Hoffmann U, Patel MR et al (2015) Outcomes of anatomical versus functional testing for coronary artery disease. N Engl J Med 372:1291–1300
9. Versteylen MO, Kietselaer BL, Dagnelie PC et al (2013) Additive value of semiautomated quantification of coronary artery disease using cardiac computed tomographic angiography to predict future acute coronary syndrome. J Am Coll Cardiol 61:2296–2305
10. Ovrehus KA, Gaur S, Leipsic J et al (2018) CT-based total vessel plaque analyses improves prediction of hemodynamic significance lesions as assessed by fractional flow reserve in patients with stable angina pectoris. J Cardiovasc Comput Tomogr 12:344–349
11. Lee SE, Park HB, Xuan D et al (2019) Consistency of quantitative analysis of coronary computed tomography angiography. J Cardiovasc Comput Tomogr 13:48–54

12. Antonopoulos AS, Sanna F, Sabharwal N et al (2017) Detecting human coronary inflammation by imaging perivascular fat. Sci Transl Med. https://doi.org/10.1126/scitranslmed.aal2658
13. Oikonomou EK, Marwan M, Desai MY et al (2018) Non-invasive detection of coronary inflammation using computed tomography and prediction of residual cardiovascular risk (the CRISP CT study): a post-hoc analysis of prospective outcome data. Lancet 392:929–939
14. Ford TJ, Ong P, Sechtem U et al (2020) Assessment of vascular dysfunction in patients without obstructive coronary artery disease: why, how, and when. JACC Cardiovasc Interv 13:1847–1864
15. Taylor AJ, Cerqueira M, Hodgson JM et al (2010) ACCF/SCCT/ACR/AHA/ASE/ASNC/NASCI/SCAI/SCMR 2010 appropriate use criteria for cardiac computed tomography. A report of the American College of Cardiology Foundation Appropriate Use Criteria Task Force, the Society of Cardiovascular Computed Tomography, the American College of Radiology, the American Heart Association, the American Society of Echocardiography, the American Society of Nuclear Cardiology, the North American Society for Cardiovascular Imaging, the Society for Cardiovascular Angiography and Interventions, and the Society for Cardiovascular Magnetic Resonance. J Am Coll Cardiol 56:1864–1894
16. Leipsic J, Abbara S, Achenbach S et al (2014) SCCT guidelines for the interpretation and reporting of coronary CT angiography: a report of the Society of Cardiovascular Computed Tomography Guidelines Committee. J Cardiovasc Comput Tomogr 8:342–358
17. Maurovich-Horvat P, Ferencik M, Voros S, Merkely B, Hoffmann U (2014) Comprehensive plaque assessment by coronary CT angiography. Nat Rev Cardiol 11:390–402
18. Motoyama S, Ito H, Sarai M et al (2015) Plaque characterization by coronary computed tomography angiography and the likelihood of acute coronary events in mid-term follow-up. J Am Coll Cardiol 66:337–346
19. Lee JM, Choi KH, Koo BK et al (2019) Prognostic implications of plaque characteristics and stenosis severity in patients with coronary artery disease. J Am Coll Cardiol 73:2413–2424
20. Chang HJ, Lin FY, Lee SE et al (2018) Coronary atherosclerotic precursors of acute coronary syndromes. J Am Coll Cardiol 71:2511–2522
21. Heo R, Park HB, Lee BK et al (2016) Optimal boundary detection method and window settings for coronary atherosclerotic plaque volume analysis in coronary computed tomography angiography: comparison with intravascular ultrasound. Eur Radiol 26:3190–3198
22. Park HB, Lee BK, Shin S et al (2015) Clinical feasibility of 3D automated coronary atherosclerotic plaque quantification algorithm on coronary computed tomography angiography: comparison with intravascular ultrasound. Eur Radiol 25:3073–3083
23. Nakazato R, Shalev A, Doh JH et al (2013) Aggregate plaque volume by coronary computed tomography angiography is superior and incremental to luminal narrowing for diagnosis of ischemic lesions of intermediate stenosis severity. J Am Coll Cardiol 62:460–467
24. Gaur S, Ovrehus KA, Dey D et al (2016) Coronary plaque quantification and fractional flow reserve by coronary computed tomography angiography identify ischaemia-causing lesions. Eur Heart J 37:1220–1227
25. Oda S, Utsunomiya D, Funama Y et al (2016) Effect of iterative reconstruction on variability and reproducibility of epicardial fat volume quantification by cardiac CT. J Cardiovasc Comput Tomogr 10:150–155
26. Yong AS, Layland J, Fearon WF et al (2013) Calculation of the index of microcirculatory resistance without coronary wedge pressure measurement in the presence of epicardial stenosis. JACC Cardiovasc Interv 6:53–58
27. Lee JM, Layland J, Jung JH et al (2015) Integrated physiologic assessment of ischemic heart disease in real-world practice using index of microcirculatory resistance and fractional flow reserve: insights from the International Index of Microcirculatory Resistance Registry. Circ Cardiovasc Interv. https://doi.org/10.1161/CIRCINTERVENTIONS.115.002857
28. Stenstrom I, Maaniitty T, Uusitalo V et al (2017) Frequency and angiographic characteristics of coronary microvascular dysfunction in stable angina: a hybrid imaging study. Eur Heart J Cardiovasc Imaging 18:1206–1213
29. Ford TJ, Stanley B, Good R et al (2018) Stratified medical therapy using invasive coronary function testing in angina: the CorMicA trial. J Am Coll Cardiol 72:2841–2855
30. Crea F, Camici PG, Bairey Merz CN (2014) Coronary microvascular dysfunction: an update. Eur Heart J 35:1101–1111
31. Camici PG, d'Amati G, Rimoldi O (2015) Coronary microvascular dysfunction: mechanisms and functional assessment. Nat Rev Cardiol 12:48–62
32. Taqueti VR, Di Carli MF (2018) Coronary microvascular disease pathogenic mechanisms and therapeutic options: JACC state-of-the-art review. J Am Coll Cardiol 72:2625–2641
33. Siasos G, Sara JD, Zaromytidou M et al (2018) Local low shear stress and endothelial dysfunction in patients with nonobstructive coronary atherosclerosis. J Am Coll Cardiol 71:2092–2102
34. Vergallo R, Papafaklis MI, Yonetsu T et al (2014) Endothelial shear stress and coronary plaque characteristics in humans: combined frequency-domain optical coherence tomography and computational fluid dynamics study. Circ Cardiovasc Imaging 7:905–911
35. Yamamoto E, Siasos G, Zaromytidou M et al (2017) Low endothelial shear stress predicts evolution to high-risk coronary plaque phenotype in the future: a serial optical coherence tomography and computational fluid dynamics study. Circ Cardiovasc Interv. https://doi.org/10.1161/CIRCINTERVENTIONS.117.005455
36. Milanese G, Silva M, Ledda RE et al (2020) Validity of epicardial fat volume as biomarker of coronary artery disease in symptomatic individuals: results from the ALTER-BIO registry. Int J Cardiol 314:20–24
37. Nappi C, Ponsiglione A, Acampa W et al (2019) Relationship between epicardial adipose tissue and coronary vascular function in patients with suspected coronary artery disease and normal myocardial perfusion imaging. Eur Heart J Cardiovasc Imaging 20:1379–1387
38. Fearon WF, Balsam LB, Farouque HM et al (2003) Novel index for invasively assessing the coronary microcirculation. Circulation 107:3129–3132
39. Lee BK, Lim HS, Fearon WF et al (2015) Invasive evaluation of patients with angina in the absence of obstructive coronary artery disease. Circulation 131:1054–1060
40. Kobayashi Y, Lee JM, Fearon WF et al (2017) Three-vessel assessment of coronary microvascular dysfunction in patients with clinical suspicion of ischemia: prospective observational study with the index of microcirculatory resistance. Circ Cardiovasc Interv. https://doi.org/10.1161/CIRCINTERVENTIONS.117.005445
41. Echavarria-Pinto M, van de Hoef TP, Nijjer S et al (2017) Influence of the amount of myocardium subtended to a coronary stenosis on the index of microcirculatory resistance. Implications for the invasive assessment of microcirculatory function in ischaemic heart disease. EuroIntervention 13:944–952

42. Murai T, Lee T, Yonetsu T et al (2013) Variability of microcirculatory resistance index and its relationship with fractional flow reserve in patients with intermediate coronary artery lesions. Circ J 77:1769–1776
43. Sugiyama T, Kanaji Y, Hoshino M et al (2020) Determinants of pericoronary adipose tissue attenuation on computed tomography angiography in coronary artery disease. J Am Heart Assoc. https://doi.org/10.1161/JAHA.120.016202

Publisher's note Springer Nature remains neutral with regard to jurisdictional claims in published maps and institutional affiliations.